Available online at www.sciencedirect.com

ScienceDirect

journal homepage: www.elsevier.com/locate/he
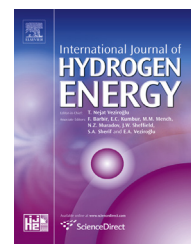
Modeling of a Vanadium Redox Flow Battery for power system dynamic studies

Leonardo J. Ontiveros*, Pedro E. Mercado

Consejo Nacional de Investigaciones Científicas y Técnicas (CONICET) — Instituto de Energía Eléctrica (IEE), Facultad de Ingeniería de la Universidad Nacional de San Juan (UNSJ), San Juan, CP 5400, Argentina

ARTICLE INFO

ABSTRACT

Vanadium Redox Flow Battery (VRB) is an electrochemical energy storage system based on a reversible chemical reaction within a sealed electrolyte. Several models have been developed which now offer a good understanding of the VRB operating principles; this knowledge is important to evaluate its performance when applied in power systems. However, these models depend on parameters that are difficult to obtain experimentally or in data sheets. In this regard, this article presents a new VRB model based on the stack efficiency curves, usually determined by the manufacturer. This model is especially useful for computing intensive applications, such as power system dynamic studies, in order to maintain a low run-time. Finally, the simulation results obtained through the proposed model are compared with laboratory results of an experimental VRB system, showing a striking resemblance with only a little relative error arising from them.

1. Introduction

The motivation behind developing electrical equivalent models for batteries stems from an interest in studying their application in power systems. There are several ongoing studies related to the use of energy storage in power systems. Many authors have seen potential for short-term and long-term storage devices based on the latest developments in storage technologies, one of which is the Vanadium Redox Flow Battery (VRB) [1].

As regards wind energy systems, there is a growing interest in using storage devices for power smoothing, load levelling application and eventually frequency control. The addition of energy storage in wind farms provides a smooth output power by acting as a source or sink of real power [2]. Furthermore, it provides an improved transient response, as well as a potential for aiding frequency and voltage regulation. The following characteristics are desirable in a storage system for wind applications: long term storage, operation over a wide range of outputs, high efficiency, low maintenance, long life and fast response to rapid changes. These requirements are met by VRB technology.

Several models have been found in the literature: in Ref. [1] the author develops a complete VRB model, which takes into account the voltage losses and mechanical losses, but it does not consider the parasitic current losses; additionally, this model depends on parameters that are difficult to obtain from data sheets. The model presented in Ref. [2] is less complex, but it ignores the nonlinearity of the stacks. The work presented in Ref. [3] focuses on the modeling of the VRB near practical operating setups; however the model is not accurate during the transient response. Unlike other models, this paper presents a new VRB model based on the stack efficiency

curves given by the manufacturer. Moreover, it includes an improved mechanical model developed in Ref. [1], so that the complete VRB model is finally obtained. Then, simulation results obtained through the new developed model are compared with those from both the models of [1] and the experimental VRB system built in Ref. [4]. This comparison shows a great accuracy of the new model, and the results obtained present only a little relative error with respect to the experimental ones.

2. The Vanadium Redox Flow Battery

The VRB is an electrochemical energy storage system which converts chemical energy into electrical energy and vice versa. The general scheme of the VRB is shown in Fig. 1. It consists of two electrolyte tanks, containing sulphuric acid electrolyte with active vanadium species in different oxidation states: V_4/V_5 redox couple (positive) and V_2/V_3 redox couple (negative). Both electrolytes are circulated through the cell stack by pumps. The stack consists of many cells, each of which contains two half-cells that are separated by a proton exchange membrane (PEM). In the half-cells the electrochemical reactions take place on inert carbon felt polymer composite electrodes from which an external direct current is used, in order to charge or discharge the battery.

In VRB, two simultaneous reactions occur on both sides of the membrane, as illustrated in Fig. 2. During the discharge, electrons are removed from the negative electrolyte (anolyte) and transferred through the external circuit to the positive electrolyte (catholyte). The flow of electrons is reversed during the charge; the reduction takes place in the anolyte and the oxidation in the catholyte [1].

A single cell produces a nominal potential of approximately 1.35 V, depending on the concentration of vanadium. The terminal voltage is achieved by series connection of many cells into a "stack". The amount of available power is related to the stack voltage and the current density established through
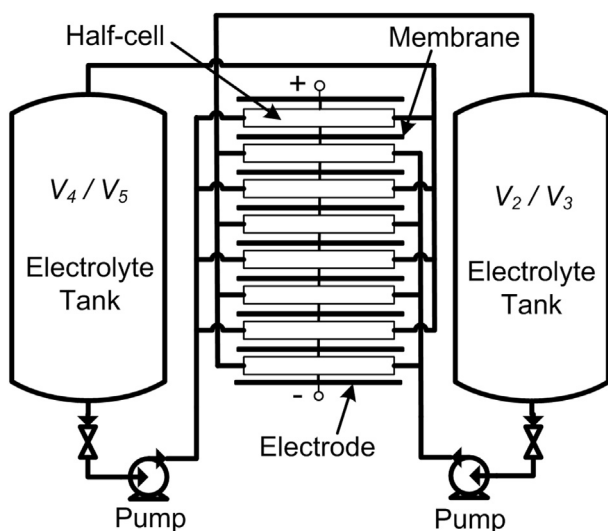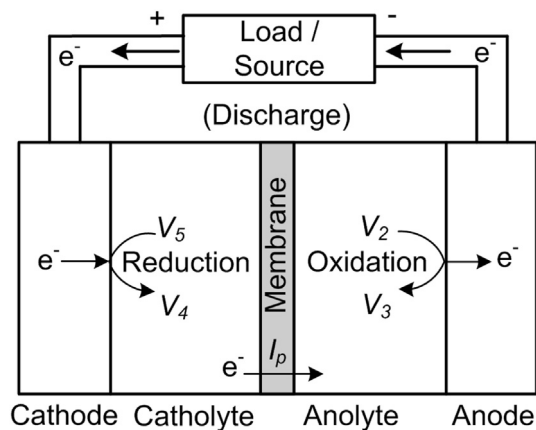

Fig. 2 – **Reactions in the proton exchange membrane (PEM).**

the cell, while the available energy only depends on the supply of the charged electrolyte into the stack. So, the rated power and the stored energy can be readily upgraded by increasing or decreasing the stack and the electrolyte tank, respectively.

3. An existing electrochemical model of the VRB stack

In Ref. [1], a complete model of the VRB is presented, which is made up of two parts: the electrochemical model and the mechanical model. The electrochemical model describes the behavior of the stack; mainly it depicts how the stack voltage (U_{stack}) depends on the operating conditions, i.e., the stack current (I_{stack}), the vanadium concentrations in the electroactive cells c_{av}, the protons concentration c_{H+}, the electrolyte flowrate Q, and the temperature T. Furthermore, it also describes how the electrolyte compositions change while the battery is operating. The schematic representation of this model is shown in Fig. 3, which is composed of six subsystems. Each of them is described below:

3.1. Stack voltage

The stack voltage U_{stack} depends on the equilibrium voltage U_{eq} and the voltage losses U_{loss}; the equilibrium conditions are met when no current is flowing through the stack. On account of the membrane resistance high value, the parasitic current is low and there are minimum voltage losses. Thus, U_{stack}
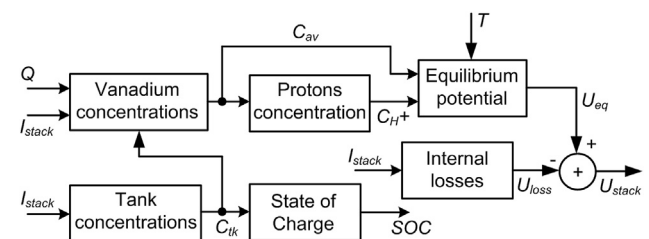

Fig. 1 – **General Scheme of a Vanadium Redox Flow Battery.**

Fig. 3 – **Schematic representation of the stack presented in Ref. [1].**

equals U_{eq}; otherwise the voltage losses modify U_{stack}. Note that the sign of U_{loss} depends on the stack current direction (charge or discharge) [1]. Hence U_{stack} is determined by:

$$U_{stack} = U_{eq} - U_{loss} \tag{1}$$

The equilibrium voltage corresponds to the sum of the equilibrium potential of the individual cells composing the stack ($U_{eq,cell}$). This potential is set by the Nernst equation [1] and hinges on the concentration of the vanadium ions (3).

$$U_{eq} = \sum_{1}^{N_{cell}} U_{eq,cell} \tag{2}$$

$$U_{eq,cell} = U_0' + \frac{RT}{F} \ln\left[\left(\frac{c_{av5}c_{H+}}{c_{av4}}\right)\left(\frac{c_{av2}}{c_{av3}}\right)\right] \tag{3}$$

where U_0' is the standard cell potential, R is the gas constant and F is the Faraday constant, c_{avi} is the mean value of the vanadium concentration for each vanadium species, as c_{H+} is the proton concentration. The characteristic curve of the equilibrium potential $U_{eq,cell}$ is illustrated in Fig. 4 for a single cell, as a function of the state of charge (SOC). In practice, the SOC is limited between 0.1 and 0.9 pu, due to over voltage issues on charging, and under voltage issues on discharging.

3.2. Voltage losses

When an external current flows through the stack, the equilibrium conditions are not met anymore and the stack voltage U_{stack} is now determined by the difference between the equilibrium potential U_{eq} and the voltage losses U_{loss}, in accordance with (1) [1]. These losses are often called overpotentials and they represent the energy needed in order to force the redox reaction for proceeding at required rate (4).

$$U_{loss}(t) = U_{act}(t) + U_{conc}(t) + U_{ohm}(t) + U_{ion}(t) \tag{4}$$

The activation U_{act} and the concentration U_{conc} overpotentials are electrode phenomena; U_{act} is associated with the energy required for initiating a charge transfer, and U_{conc} ari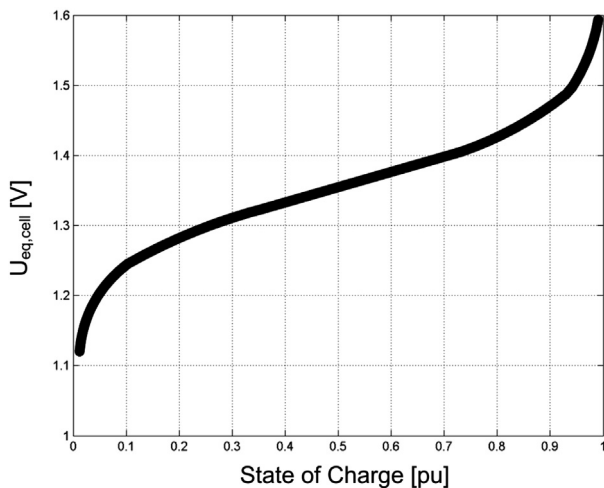ses from the differences in concentration between the bulk solution and the electrode surface. In addition, the ohmic U_{ohm} and ionic U_{ion} losses also alter the stack voltage. The ohmic losses U_{ohm} are caused by the electric resistance of the electrodes, bipolar plates and the collector plates. The ionic losses U_{ion} occur in the electrolytes and the membrane, and are caused by the resistance to the passage of an ionic flow.

3.3. Concentration of vanadium ions

Although the ions concentrations are not uniformly distributed inside the cells, the mean value c_{avi} is used as an approximation in the Nernst equation (3). The vanadium concentrations c_{avi} are related to their initial tank concentration c_{tki0}, the volume of the reservoir V_{tk}, the number of cells N_{cell}, the stack current I_{stack} and the electrolyte flowrate Q [1]:

$$c_{avi(t)} = c_{tki0} + \frac{bN_{cell}}{V_{tk}eN_A}\int I_{stack}(t)dt + \frac{bN_{cell}I_{stack}(t)}{2eN_AQ(t)} \tag{5}$$

where b is a sign factor depending on the considered vanadium species (-1 for V_2 and V_5 ions, and $+1$ for V_3 and V_4 ions), N_A is the Avogadro number and e is the elementary charge. It is interesting to note that the sum of the first two terms corresponds to the concentration in the tank c_{tki}, and that by definition the current is positive during the discharge.

3.4. Concentration of protons

The protons concentration in the catholyte depends on the electrolyte composition and varies with the state of charge [1]:

$$c_{H+} = c_{H+,disch} + c_{av5} \tag{6}$$

where $c_{H+,\ disch}$ is the proton concentration when the electrolyte is completely discharged.

3.5. State of charge

The state of charge SOC indicates how much energy is stored in the battery; it varies from 0 (discharged state) to 1 (charged).
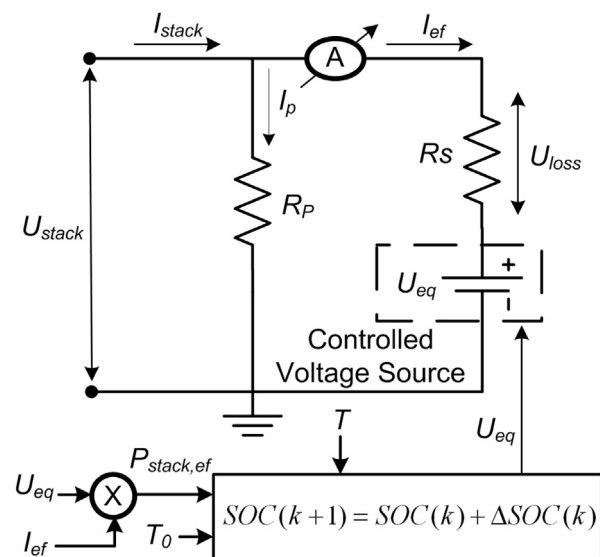

Fig. 4 − Equilibrium cell voltage versus state of charge at 25 °C.

Fig. 5 − A new model of the VRB stack.

When neglecting the small variation of the SOC with the protons concentration, its value is defined by the following relation:

$$\text{SOC} = \frac{c_{tk2}}{c_{tk2} + c_{tk3}} = \frac{c_{tk5}}{c_{tk4} + c_{tk5}} \tag{7}$$

In general, the models observed in the literature do not consider the parasitic current losses; what is more, these models depend on parameters that are difficult to obtain from data sheets or experimentally. In the light of these considerations, a new VRB model is presented in the following chapter.

4. A new model of the VRB stack

The VRB stack model presented in this paper improves that one presented in Refs. [1] [2], taking into account the voltage losses and the parasitic current losses with the resistances Rs and Rp respectively (Fig. 5). The model calculates the equilibrium voltage (U_{eq}), the stack voltage (U_{stack}) and the state of charge (SOC) of the electrolyte.

4.1. State of charge

The SOC represents the percentage of active vanadium species in the electrolyte. In this case, the SOC is modelled as a state variable which is calculated at each sample period (To) [2]. According to (8), the SOC at the instant k depends on the energy stored $E(k)$, and the maximum energy capacity E_{max} [5–7]:

$$\text{SOC}(k) = \frac{E(k)}{E_{max}} \tag{8}$$

The SOC in the next sample period is:

$$\text{SOC}(k+1) = \text{SOC}(k) + \Delta\text{SOC}(k) \tag{9}$$

Unlike the models developed in Refs. [2,5–7], this paper establishes that only the effective stack power $P_{stack,ef}(k)$ affects the SOC; otherwise the SOC is overestimated during the charge and discharge cycles. Thus, the variation of the state of charge (ΔSOC) is calculated with (10):

$$\Delta\text{SOC}(k) = \frac{\Delta E(k)}{E_{max}} = \frac{-U_{eq}(k)I_{ef}(k)To}{E_{max}} \tag{10}$$

where $I_{ef}(k)$ is the effective current of the VRB cells stack without the parasitic current losses I_p. The term $U_{eq}(k)^* I_{ef}(k)$ is the effective stack power $P_{stack,ef}(k)$. To is the sample period.

4.2. Stack voltage

The cell equilibrium potential is directly related to the state of charge as shown in (11) [2,7–10].

$$U_{eq,cell} = U_0 + \frac{2RT}{F}\ln\left(\frac{\text{SOC}}{1 - \text{SOC}}\right) \tag{11}$$

where U_0 is the internal cell voltage when the SOC is 0.5 pu. The equilibrium voltage (U_{eq}) is calculated with (2).

4.3. Voltage losses

The voltage losses presented in (4) are difficult to identify and measure. Therefore, an equivalent resistance is used instead:

$$U_{loss} = RsI_{ef} \tag{12}$$

where Rs is the equivalent charge/discharge resistance, this value is found experimentally and includes polarization resistances as well as ohmic resistances.

4.4. Parasitic current losses

The parasitic current losses (or coulombic losses) can be caused by side reactions, such as oxygen or hydrogen evolution that might occur during the charge. The cross mixing of the electrolyte through the membrane due to ion transfer and unbalanced flowrate of the electrolyte are other source of coulombic losses [11]. The parasitic current I_p considers the coulombic losses of the stack:

$$I_p = \frac{U_{stack}}{Rp} \tag{13}$$

4.5. Stack energy efficiency

The voltage and coulombic losses lead to stack energy efficiency below 1. By definition, the stack efficiency is the relationship between the energy drawn by the VRB system during the charge cycle, and the energy delivered by the system during the discharge cycle (14). In order to calculate the exact efficiency, the SOC at the beginning of the charge cycle (t_0) must be equal to the SOC at the end of the discharge cycle (t_2) (Fig. 6); otherwise the VRB system stores or delivers energy after the charge/discharge process.

$$\eta_e = \frac{|E_{stack,disch}|}{|E_{stack,charge}|} = \frac{\int_{t_1}^{t_2} |P_{stack,disch}| \cdot dt}{\int_{t_0}^{t_1} |P_{stack,charge}| \cdot dt} \tag{14}$$
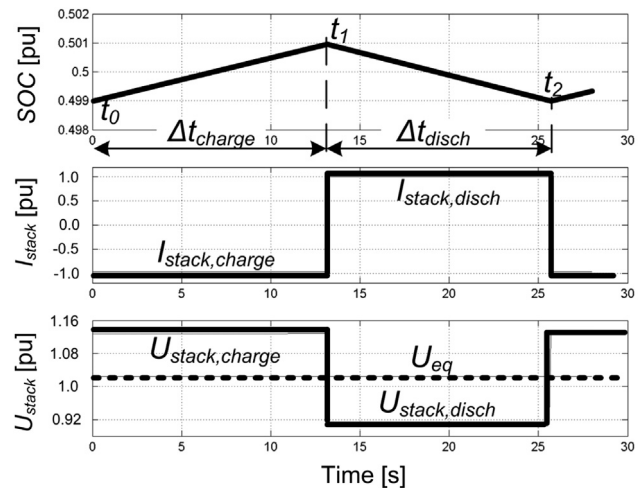

Fig. 6 – **Charge/discharge cycle of the experimental stack.**

$$\eta_e = \frac{\int_{t_1}^{t_2} U_{stack,disch} \cdot |I_{stack,disch}| \cdot dt}{\int_{t_0}^{t_1} U_{stack,charge} \cdot |I_{stack,charge}| \cdot dt} \tag{15}$$

The papers presented in Refs. [2,4,9–12] demonstrate in an experimental way, that the voltage and coulombic efficiency for a specific stack depends on the stack current operation. Fig. 7 shows that the coulombic efficiency (η_c) increases and voltage efficiency (η_v) decreases with increasing current giving maximum overall energy efficiency (η_e) of 0.8 when the stack current is approximately 0.6 pu.

In order to evaluate the stack efficiency during a complete cycle, the stack current is set constant during the charge and discharge process; otherwise a variable stack current affects the value of the energy efficiency (Fig. 7). So, the energy efficiency value depends only on the stack voltage and the integration period. If the charge and discharge periods tend to zero (Fig. 6), the stack voltage remains constant during the integration period, hence (15) becomes (16).

$$\eta_e = \frac{\int_{t_1}^{t_2} U_{stack,disch} \cdot dt}{\int_{t_0}^{t_1} U_{stack,charge} \cdot dt} = \frac{\lim_{t_2 \to t_1} \int_{t_1}^{t_2} U_{stack,disch} \cdot dt}{\lim_{t_1 \to t_0} \int_{t_0}^{t_1} U_{stack,charge} \cdot dt} \tag{16}$$

$$\eta_e = \frac{U_{stack,disch} \Delta t_{disch}}{U_{stack,charge} \Delta t_{charge}} = \eta_v * \eta_c \tag{17}$$

Equation (17) denotes that the energy efficiency is the product between the voltage efficiency (η_v) and the coulombic efficiency (η_c). So, the voltage efficiency is defined as the division of the stack voltage during the discharge by the stack voltage during the charge:

$$\eta_v = \frac{U_{stack,disch}}{U_{stack,charge}} \tag{18}$$

In the same way, the coulombic efficiency is determined as the division of the amperes-hours delivered during the discharge by the amperes-hours drawn during the charge. When the VRB operates at constant charge/discharge current, the coulombic efficiency is easily calculated with (19):

$$\eta_c = \frac{|I_{stack,disch}| \Delta t_{disch}}{|I_{stack,charge}| \Delta t_{charge}} = \frac{\Delta t_{disch}}{\Delta t_{charge}} \tag{19}$$

In Fig. 5, the controlled voltage source U_{eq} represents the model of the VRB stack without the coulombic and voltage losses. In this sub-system, the energy delivered is equal to the energy absorbed by the VRB system:

$$U_{eq} I_{ef,charge} \Delta t_{charge} = U_{eq} I_{ef,disch} \Delta t_{disch} \tag{20}$$

From (19) and (20), the coulombic efficiency is set by:

$$\eta_c = \frac{\Delta t_{disch}}{\Delta t_{charge}} = \frac{I_{ef,charge}}{I_{ef,disch}} = f_c(I_{stack}) \tag{21}$$

The main component of the coulombic losses is the diffusion of ions across the membrane. Therefore, the parasitic current I_p depends on the stack current I_{pstack}. In this work, an ohmic resistance (Rp) is employed as an approximation of the parasitic losses. So, the ratio between the stack voltage U_{stack} and the parasitic current I_p remains constant and equal to Rp, for either the charging or discharging process (22). Therefore, the quotient between the parasitic current during the discharge $I_{p,disch}$ and the parasitic current during the charge $I_{p,charge}$ is equal to voltage efficiency η_v (23):

$$Rp = \frac{U_{stack,disch}}{I_{p,disch}} = \frac{U_{stack,charge}}{I_{p,charge}} \tag{22}$$

$$\eta_v = \frac{U_{stack,disch}}{U_{stack,charge}} = \frac{I_{p,disch}}{I_{p,charge}} = f_v(I_{stack}) \tag{23}$$

4.6.   Determination of the stack parameters

The stack parameters (Rs, Rp) are obtained using the model presented in Fig. 5. Equations (24)–(27) describe the charge and discharge process of the VRB stack:

$$U_{stack,charge} = U_{eq} + I_{ef,charge} Rs \tag{24}$$

$$I_{stack,charge} = I_{ef,charge} + I_{p,charge} \tag{25}$$

$$U_{stack,disch} = U_{eq} - I_{ef,disch} Rs \tag{26}$$

$$I_{stack,disch} = I_{ef,disch} - I_{p,disch} \tag{27}$$

The stack parameters Rs and Rp are obtained solving (21), and (23)–(27):

$$Rs = \frac{U_{eq}}{I_{stack}} \frac{(1 - \eta_v)}{(1 + \eta_v)} \tag{28}$$

$$Rp = \frac{U_{eq}}{I_{stack}} \frac{(1 + \eta_c)}{(1 - \eta_c)} \tag{29}$$

Fig. 7 shows that the coulombic and voltage efficiencies vary with the stack current, so Rs and Rp are not constant. Instead of solving the circuit presented in Fig. 5, a new method that calculates two gains is proposed here, so as to obtain the stack voltage U_{stack} and the effective current I_{ef}. These
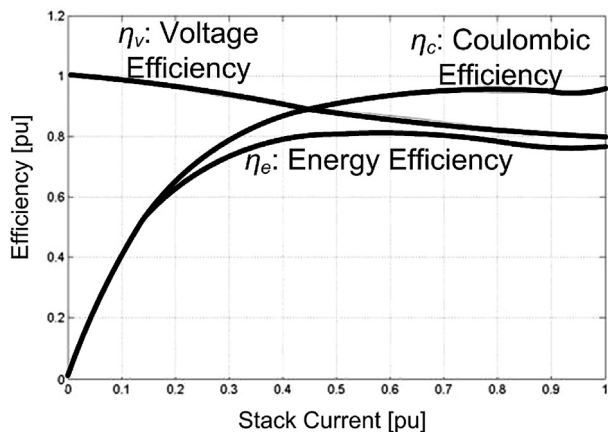

Fig. 7 – **Voltage, coulombic and energy efficiencies of the VRB stack.**

parameters are the voltage and current gains (K_v, K_c) and they are obtained by solving the equations system (24)–(29). Note that K_c and K_v gains depend on the stack current, the experimental efficiency curves (η_v, η_c) and the operating condition (charge or discharge):

$$K_{c,\text{charge}(I_{\text{stack}})} = \eta_c K_{c,\text{disch}(I_{\text{stack}})} = \eta_c \frac{(1 + \eta_v)}{(1 + \eta_e)} \tag{30}$$

$$K_{v,\text{charge}(I_{\text{stack}})} = \frac{K_{v,\text{disch}(I_{\text{stack}})}}{\eta_v} = \frac{(1 + \eta_c)}{(1 + \eta_e)} \tag{31}$$

Hence, the effective stack current and the terminal stack voltage are obtained with (32) and (33):

$$I_{\text{ef}} = K_{c(I_{\text{stack}})} I_{\text{stack}} \tag{32}$$

$$U_{\text{stack}} = K_{v(I_{\text{stack}})} U_{\text{eq}} \tag{33}$$

During the charge process, the voltage gain K_v is greater than 1 and the current gain K_c is lower than 1. Thus, the terminal voltage is greater than the equilibrium voltage and the effective current is lower than the stack current, as it is expected. This situation is reversed during the discharge process, since the voltage gain K_v is lower than 1, and the current gain K_c is greater than 1. In conclusion, the knowledge of the stack efficiency curves leads to the new model of the VRB stack showed in Fig. 8. Usually, the VRB stack provides a cell connected to the hydraulic circuit, but it is electrically isolated, in order to measure the open circuit voltage and the SOC.

5. Mechanical model

The work presented in Ref. [1] develops the mechanical model of the VRB system. This model is composed of an analytical part that models the pipes, bends, valves, tanks and pumps, and a numerical part obtained from a finite element method that describes the more complex stack hydraulic circuit. The mechanical model calculates the total power consumption of the pumps ($P_{2\text{pump}}$) which are caused by the electrolyte flowrate. In addition to the mechanical model, in this paper it is suggested to incorporate the equivalent dc current consumption of the pumps (I_{pump}). Therefore, the value of I_{pump} represents the mechanical losses of the VRB system (34).

$$I_{\text{pump}} = \frac{P_{2\text{pumps}}}{U_{\text{stack}}} \tag{34}$$

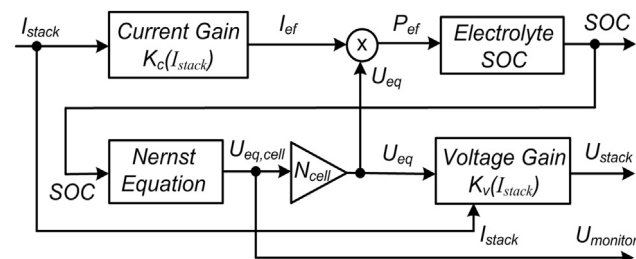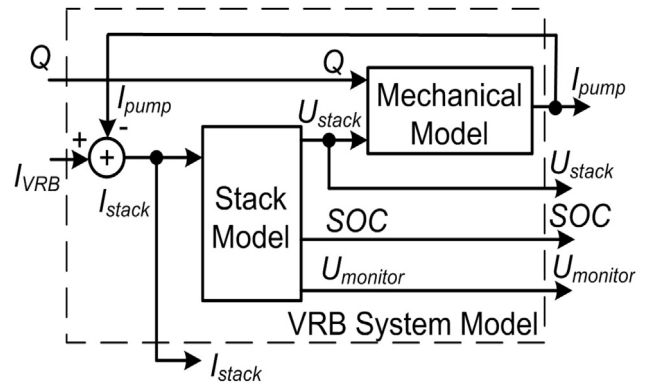Fig. 8 – Schematic representation of the improved VRB model based on the stack efficiency.

Fig. 9 – Complete model of the VRB System.

6. VRB system model

The combination of the stack model and mechanical models leads to the complete VRB model as illustrated in Fig. 9. This model is a powerful tool for understanding the behaviour of VRB, for identifying and quantifying the losses in the storage system, and finally enhancing the overall efficiency.

The terminal VRB current I_{VRB} determines the stack current I_{stack} and consequently, the terminal stack voltage U_{stack} and the state of SOC charge of the electrolyte. The external control system sets the flowrate Q producing a pressure drop in the hydraulic system; the required energy to pump the electrolyte is provided by two dc machines. So, the pump current consumption I_{pump} is subtracted from the terminal current I_{VRB} so as to obtain the stack current I_{stack}.

7. Simulation results

In this section, the results obtained with both the proposed model of the VRB stack and the electrochemical model developed in Ref. [1], is compared with those of the experimental system built by M. Skyllas Kazacos [4]. The characteristics of the experimental system are summarized in Table 1. The voltage profile of this system during the charge process at 100 A is illustrated in Fig. 10. At t = 1.5 h, the stack current is reversed and consequently the VRB is discharged, causing a voltage drop. In Fig. 10, the dotted curve corresponds to the

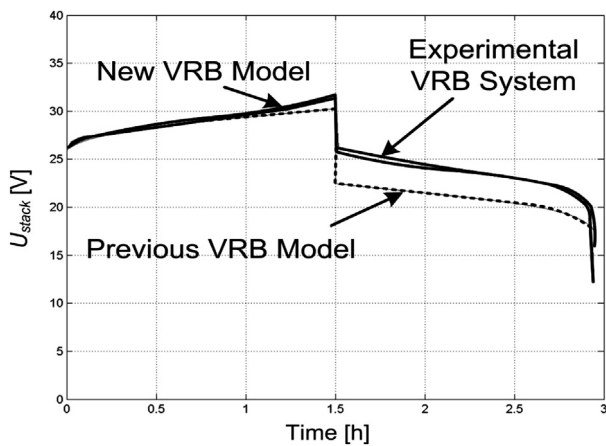| Table 1 – Characteristics of the experimental VRB system.	
Name	Value
Number of cells	19
Number of stacks	2
Electrolyte flowrate	1.97 l/s
Vanadium Concentration	2 mol/l
Tank size	83 l
Maximum stack Current	120 A
Average power	2.5 kW
Storage capacity	5 kWh

Fig. 10 — VRB voltage profile at a constant charge/discharge current of 100 A.
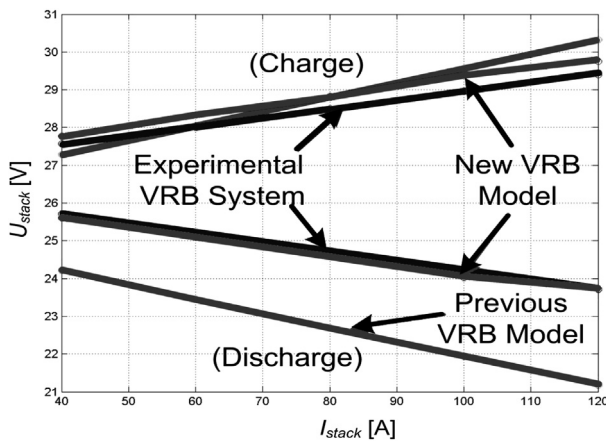

Fig. 11 — Polarization curves for the VRB system at 0.5 SOC.

electrochemical model obtained in Ref. [1] and the solid curve to the new model of the VRB stack proposed here.

Fig. 10 reveals that the new model of the VRB stack offers a good approximation to the real system; the relative error is less than 2%. The incorporation of the voltage losses and parasitic current losses in the model leads to a more accurate calculation of the SOC. Unlike the model presented in Ref. [1],

Table 2 — Parameters of the stack	
Symbol	Value
$c_{H+,\ disch}$	6 mol/l
E_{max}	5 kWh
F	9.6485 C/mol
N_A	6022×10^{23} mol^{-1}
R	83144 V C/mol K
Rs	0.038 Ω
T	29815 K
U_0'	1.255 V
U_0	1.41 V
V_{tk}	83 l

the new model predicts the voltage collapse which occurs at the end of the experiment (Fig. 10).

7.1.   Polarization curves

The terminal voltage of the VRB system is evaluated at 0.5 SOC, for each value of the stack current (charge and discharge). Fig. 11 shows that the polarization curves of the new suggested model are very similar to the experimental curves, especially at the discharge. The maximum relative error is 1.55%.

8.   Conclusions

This article presents a new VRB model based on stack efficiency curves. The complete model of the VRB system is obtained including the mechanical model of the VRB hydraulic circuit and pumps. The results of an experimental VRB system are compared with those of the new model by employing digital simulations. The comparison shows high similarity between them, with a relative error less than 2%. The advantages of the suggested model are that: 1) it does not depend on parameters that are difficult to obtain from data sheets, 2) the stack efficiency curves are easier to obtain either experimentally or by the manufacturer, 3) the model takes into account both the voltage and coulombic losses of the stack, so the performance of the model has a high degree of accuracy, 4) the proposed model can be employed for applications which incorporate electrochemical energy storage systems.

The proposed improved mechanical model is important for assessing the power required in order to flow the electrolytes. Its combination with the implied stack model is useful in order to represent the operation of a VRB system considering also the associated losses, which can be now identified and quantified. So, the complete model offers a powerful tool for understanding the VRB behaviour, and, consequently, for enhancing its performance with adequate control strategies.

Appendix

The stack parameters are given in Table 2. Table 3 shows the values of the coulombic and voltage efficiency.

REFERENCES

[1] Blanc C, Ruffer A. Multiphysics and energetic modeling of a vanadium redox flow battery. In: Proc. international conference on sustainable energy technologies (ICSET), Singapore October 2008. pp. 759—64.

Table 3 — Coulombic and voltage efficiency data		
I_{stack} [pu]	η_c	η_v
0	0	1.0
0.333	0.8255	0.9218
0.5	0.9138	0.8862
0.666	0.9452	0.8551
0.833	0.9468	0.8172
1.0	0.964	0.7978

[2] Chahwan J, Abbey C, Joos G. VRB modelling for the study of output terminal voltages, internal losses and performance. In: Proc. electric power conference (EPC), Montreal, Canada October 2007. pp. 387–92.

[3] Li M, Funaki T, Hikihara T. A study of output terminal voltage modeling for redox flow battery based on charge and discharge experiments. In: Proc. power conversion conference (PCC), Nagoya, Japan April 2007. pp. 221–5.

[4] Skyllas-Kazacos M, Menictas C. The vanadium redox battery for emergency back-up applications. In: Proc. Telecommunications energy conference (INTELEC), Melbourne, Australia October 1997. pp. 463–71.

[5] Wang W, Ge B, Bi D, Sun D. Grid-connected wind farm power control using VRB-based energy storage system. In: Proc. energy conversion congress and exposition (IEEE/ECCE) Int. Conf., Delft, Netherlands August 2010. pp. 3772–7.

[6] Chen Z, Ding M, Su J. Modeling and control for large capacity battery energy storage system. In: Proc. electric utility deregulation and restructuring and power technologies (DRPT) Int. Conf., Weihai, China July 2011. pp. 1429–36.

[7] Qiu X, Nguyen T, Crow ML, Elmore AC, McMillin B. Computer models for microgrid application. In: Proc. power and energy society general meeting (IEEE/PES) Int. Conf., Detroit, USA July 2011. pp. 1–8.

[8] Biao M, Buhan Z, Bingyin W, Guanglong X. Studies on security capacity of wind farms containing VRB energy storage system. In: Proc. electric utility deregulation and restructuring and power technologies (DRPT) Int. Conf., Weihai, China July 2011. pp. 1704–8.

[9] Wang G, Ciobotaru M, Agelidis VG. Minimising output power fluctuation of large photovoltaic plant using vanadium redox battery storage. In: Proc. power electronics, machines and drives (IET/PEMD) Int. Conf., Bristol, UK March 2012. pp. 1–6.

[10] Wang G, Ciobotaru M, Agelidis VG. PV power plant using hybrid energy storage system with improved efficiency. In: Proc. power electronics for distributed generation systems (IEEE/PEDG) Int. Conf., Aalborg, Denmark June 2012. pp. 808–13.

[11] Mousa A. Chemical and electrochemical studies of V(III) and V(II) solutions in sulfuric acid solution for vanadium battery applications. PhD thesis. Australia: The University of South Wales; 2003.

[12] Tsuda I, Kurokawa K, Nozaki K. Development of intermittent redox flow battery for PV system. In: Proc. world conference on photovoltaic energy conversion (WCPEC), Honolulu, Hawaii December 1994. pp. 946–9.